A review of Ni and Co incorporation during talc synthesis: Applications to crystal chemistry, industrial compounds and natural Ni- and Co-rich ore

François Martin, Cyril Aymonier, Sandra Einloft, Christel Carême, Mathilde Poirier, Marie Claverie, Manoela Argenton Prado, Guilherme Dias, Cyril Quilfen, Guillaume Aubert, et al.

A review of Ni and Co incorporation during talc synthesis: applications to crystal chemistry, industrial compounds and natural Ni- anc Co-rich ore.

François Martin [(1)], Cyril Aymonier [(2)], Sandra Einloft [(3)], Christel Carême [(4)], Mathilde Poirier [(1)], Marie Claverie [(1, 2, 4)], Manoela Argenton Prado [(1, 3)], Guilherme Dias [(1, 3)], Cyril Quilfen [(2)], Guillaume Aubert [(2)], Pierre Micoud [(1)], Christophe Le Roux [(1)], Angela Dumas [(1)], & Suzanne Fery-Forgues [(5)]

(1) GET UMR 5563 CNRS-UPS, Université de Toulouse III, OMP, ERT Géomatériaux, 14 Avenue Édouard Belin, 31400 Toulouse, France, francois.martin@get.omp.eu

(2) ICMCB UMR 5026 CNRS, Université de Bordeaux, 33600 Pessac, France, cyril.aymonier@icmcb.cnrs.fr

(3) Faculdade de Química (FAQUI) – Pontifícia Universidade Católica do Rio Grande do Sul (PUCRS). Porto Alegre, Brasil, Einloft@pucrs.br

(4) IMERYS, 2 place Édouard Bouillères, 31100 Toulouse, France, Christel.Careme@imerys.com

(5) SPCMIB UMR 5068 CNRS-UPS, Université Toulouse III, 118, route de Narbonne –Bât 2R1 31062 Toulouse Cedex 09 France, sff@chimie.ups-tlse.fr

Keywords: Ni, synthesis, talc, materials, crystal growth

Abstract:

This article is rather a broad review that presents the main results of studies on mineral syntheses incorporating Ni and Co cations, the interest of developing materials of this type, and some applications where these mineral materials are used as mineral filler. A reflection is then conducted to show that the mineral synthesis rich in Ni and Co makes minerals appear very similar to those found in Ni- and Co-rich lateritic environment. The studies of these lateritic natural environments can provide information on the formation processes of synthetic minerals, and conversely. These two thematic fields will be able to cross-check their data and allow to solve, for example, the chemical fractionation problems encountered in these lateritic environments.

Introduction :

Clays are abundant and cheap resources distributed worldwide, which find applications in many different fields as mineral fillers to reduce production cost and/or gain new properties in ceramic, polymer, paper, cosmetic, pharmaceutical, oil drilling and isolation industries (Kloprogge et al., 1999). Among T-O-T phyllosilicates, talc is the less complex with the formula $Mg_3Si_4O_{10}(OH)_2$ and is known from the Antiquity for its softness and its whiteness in powder form. Talc deposits are well studied and the broad spectrum of talc formation conditions explains the diversity of talc ore deposits with large variations in term of color, grain size, crystallinity, lamellar-character, softness, chemical composition and the accessory minerals such as chlorite and carbonates (Zazenski et al., 1995; Robert et al., 1996; Soriano et al., 1998; 2002). However, throughout talc applications, new requirements and/or new limitations appeared such as (i) the need of talc ore purity, particularly in cosmetic and pharmacologic uses; (ii) the difficulty to disperse talc in a water medium, and (iii) the need to use submicronic

talc particles to develop polymer based nanocomposites (Usuki et al., 1993a, b; Kojima et al., 1993a, b). To satisfy these respective requirements, several possible ways were put forward: (i) the need of high purity talc was solved by the exploration of new highly pure talc deposit (Misch et al., 2018) and/or the improvements of techniques to purify talc ore (Baba et al., 2015; Castillo et al., 2014; Dumas et al., 2015a); (ii) talc dispersion in water medium was improved by using surface treatment such as pre-coating by carboxyl methyl cellulose adsorption, for example (Bonino et al., 2002; Bacchin et al., 2006); and (iii) the need of submicronic talc particles led to the development of grinding processes such as air jet milling, sonication, stirred ball milling and dry milling (Godet, 2001). However, using these top-down approaches, the results were not as successful since natural talc is difficult to ground homogeneously below 1 μm without leading to amorphization and structural disordering (Liao and Senna, 1992; Sanchez-Soto et al., 1997; Dellisanti et al., 2009; Cavaida et al., 2015; Borges et al., 2016). In this context, in the aim to obtain the combination of the three needs (purity, nanosize without amorphization of the structure and hydrophilic character), bottom up approaches have been investigated in the last 20 years and the unique technique is the hydrothermal synthesis (Martin et al., 1992, 1996; Martin, 1994; Dumas et al., 2011a; Martin et al., 2006; Lèbre, 2007; Arseguel, 2006; Le Roux, 2010; Dumas et al., 2013a, b; Dumas, 2013c; Claverie et al., 2018). In collaboration with industrial partners (IMERYS group), the synthesis processes were recently revised and optimized to obtain a simpler, faster, and more efficient process that complies with industrial requirements. The preparation of synthetic talc requires two steps: (i) preparation of a talc precursor at room temperature with the appropriate Mg/Si talc ratio and (ii) hydrothermal treatment. Currently, synthetic talc appears in various industrial sectors as a competitive and original filler. The industrial demand for this new material will lead to a significant technology transfer this year.

However, the crystallogenesis mechanisms should be considered before scaling up the process. Although synthetic talc is a well-documented product, very little information about its precursor exists. Some authors confirmed its amorphous character and revealed a highly agglomerated and porous (micropores and mesopores) product (Dietemann, 2012; Dietemann et al., 2013; Claverie et al., 2018). Moreover, understanding synthetic talc growth mechanism is also highly applicable to understanding the crystallization of talc in natural environments ranging from low temperature (sedimentary, weathering) to high temperature (metamorphic/hydrothermal) environments.

To understand the growth mechanism, diffraction and spectroscopic methods are classically used while X-ray diffraction (XRD) data provide information about the crystalline structure at a length scale of approximately 50 Å, Fourier transform infrared spectroscopy (FTIR), for example, and X-ray absorption spectroscopy (XAS) provides details about the local structure. Extended X-ray absorption fine structure (EXAFS) was used to probe the immediate environment of the octahedral cation: the distances and coordination number (CN) of the octahedral absorbing atom. The talc synthesis procedure allows partial or complete substitution of the magnesium cation by nickel in the octahedral sheet (ionic radius of 0.69 and 0.72 Å for Ni and Mg, respectively). Because Ni atoms have more suitable energy absorption for the use of EXAFS measurements than Mg atoms (8333 and 1305 eV for Ni and Mg, respectively), synthetic Ni-talcs were used (Dumas et al., 2015b).

The aim of this note is to show the potentiality of talc nanoparticles and especially Ni- bearing talc particles. We focused on the synthesis process to obtain synthetic talc in a very short time, on the transition from proto-talc to talc using various Ni and Mg ratio in octahedral layer, and on the opportunity to use synthetic Ni-talc to measure the dispersion into polymer matrixes by monitoring the green color. Same observations may be done with Co cations, which can easily

replace Ni and Mg in TOT structure in hydrothermal synthesis.In lateritic environments, Mnoxides are commonly considered as the major Co-bearing mineral species (Dublet et al., 2017), but not TOT phases.

Synthesis process

Talc is a magnesium hydroxylated phyllosilicate (sheet silicate) of formula $Mg_3Si_4O_{10}(OH)_2$. It is the simplest pole of 2:1 type phyllosilicates. It is constituted by stacking a large number of sheets along the c* axis (Figure 1). Each sheet is composed of a hydrophilic octahedral $MgO_4(OH)_2$ layer covalently bonded to two hydrophobic SiO_4 tetrahedral layers. The 2:1 (or TOT) sheets of talc are electrically neutral and therefore no ion or water molecule is present in the interfoliar space. The sheets are connected to each other by electrostatic forces of Van der Waals type, which explain the possibility of slipping the talc sheets relative to each other when the talc is subjected to tangential shearing.

A review publication (Claverie et al., 2018) tells the history of talc synthesis since the 1950s. In summary, the first synthesis was carried out at high temperature (> 700 ° C). Until 2014, syntheses were all carried out (between 200 and 500 ° C) in hydrothermal reactors of "batch" type or closed reactors (Figure 2). The quantities of products obtained were of a few tens of grams, sufficient for crystallochemical and crystallographic studies (Chabrol et al., 2010; Dumas et al., 2013a, b; Dumas, 2013c; Martin, 1994; Martin et al., 1992, 1996, Lèbre, 2007;).

To screen the potential of synthetic talcs in some applications, the IMERYS group decided to finance a large batch reactor to obtain around one kilogram of products (Figure 3) at the end of one run. In 2015, thanks to the results obtained , the IMERYS group continued funding studies

to test other ways of manufacturing talc with the objective of producing talc in continuous mode. A process under supercritical conditions emerged as the best way to reduce synthesis times considerably, few tens of seconds while 10 hours were necessary in a closed reactor to achieve a complete production cycle(Aymonier et al., 2014). Based on the techniques developed by Aymonier's group at the ICMCB in Bordeaux (Reveron et al., 2006; Aymonier et al., 2007; Cansell et al., 2009), the consortium [ICMCB, GET and IMERYS] has developed a semi-industrial pilot facility that meets the expectations of the group and the industrial world in demand for sufficient quantities to perform tests in applications. The process takes advantage of the specific properties of water under supercritical conditions (water is neither a liquid nor a gas above 374 ° C and 221 bar). The hydrothermal reaction is indeed a precipitation reaction described in Figure 4. The principle of the hydrothermal reactor (Figure 5), which operates in continuous mode under supercritical conditions, is as follows: a precipitation reaction involving sodium metasilicate and magnesium acetate (plus acetic acid and sodium acetate) is carried out (ratio of 4Si for 3Mg in order to produce talc, for example). Then, thanks to high pressure pumps, this precipitate passes in a reactor where the conditions of the supercritical water prevail between 10 and 60 seconds maximum, conditions managed by a pressure regulator. The resulting product is then either recovered directly (followed by 3 or 4 successive washes to remove excess sodium acetate) or passed through a ceramic sinter which separates the product formed from residual sodium acetate (Dumas et al., 2016; Claverie et al., 2018).

In our example, the product obtained is talc with a basal line located at 9.6Å (Figure 6), higher than reference natural talc due to the size of the particles. The particle size of the product (Figure 7) is less than one micron with two populations centered around 90 nm and 240 nm, respectively. Transmission electron microscopy image of synthetic talc is shown in Figure 8. It is well defined and a stack of layer in c* direction (8 nm) is observed in addition to fine particles around 45 nm. Scanning electron microscopy (Figure 9) confirms the TEM observation for all

the small particles. These images in electron microscopy tell us about the morphology of the synthesized particles with strong extensions in the plane (a, b) with respect to the stacking along the axis c* (less than a dozen of sheets). Thus, the products have a high aspect ratio, which is an important physical feature for insertion into composite matrices such as polymers.

The products obtained are formed as soon as the system is in supercritical condition after very short reaction times between 10 and 60 s (Dumas et al., 2016, Claverie et al., 2018). In Figure 10, it is easy to observe that talc is formed above the supercritical conditions of water, whereas below these conditions, a poorly crystallized phase (amorphous) called proto-talc exists. The samples synthesized under supercritical conditions (TF-38023 and TF-40023) exhibit the 001, 020-110, 003, and 060-330 reflections characteristic of a talc structure. At lower temperature (TF-35020), 00ℓ reflections of talc are almost nonexistent and only 020-110 and 060-330 reflections of clays are developed. The crystallinity of the TF-40023 sample is comparable to that of the synthetic talc sample obtained in a batch reactor during 2 hours at 300°C and 85 bar. When the reaction time is reduced by half (TF-40010), talc of lower crystallinity is obtained.

The particularity of synthetic talcs in comparison with their natural counterparts is the perfect equilibrium of particles in aqueous medium. Indeed, the product obtained is in the form of an aqueous gel (Figure 11 on the right) thanks to the hydrophilic nature of synthetic talc, while the strongly hydrophobic natural talc precipitates in the same conditions. After drying and grinding, a white powder is obtained (Figure 11 on the left), which can be resuspended to reform a synthetic talc gel. This reversibility is an undeniable advantage of synthetic talc compared to natural talc.

The submicrometer-sized particles are characterized by BET values much higher (220 to 600 $m^2.g^{-1}$) than for natural talcs (maximum around 20 $m^2.g^{-1}$) , by increased exchange surfaces and by a high ratio of hydrophilic lateral borders to hydrophobic basal surfaces. The side edges are the location of silanol (SiOH) and MgOH groups. Thus, the borders have significant amounts of physisorbed water (maximum 14% determined by differential thermal gravity),which can explain the equilibrium with the aqueous medium (Figure 12) and the formation of gel.

Octahedral substitutions : From proto-talc to talc

The chemistry of the process makes it possible to replace divalent Mg atoms in part or totally by other divalent atoms such as Ni,Co, Cu, Fe and Mn. (Figure 13). Whatever the octahedral cation, the obtained products are talcs, and many studies show the solid solutions between the end-members (Ni, Mg, Fe^{2+}, …)$_3$ $Si_4O_{10}(OH)_2$ (Martin et al., 1992; Petit et al., 1995, 2004a; Corona et al., 2015). It is thus possible to obtain synthetic talc compounds colored to the core. Figure 14 shows the comparison between a natural pink talc from China (François Martin's collection), and a green synthetic talc whose Mg was replaced by Ni. The natural sample loses its color after grinding (like the colored talc samples studied by Misch et al. (2018), this talc is very pure and contains no other associated mineral which could explain the pink color, which is probably due to the arrangement of crystallites in the bulk ore inducing light reflection phenomenon) while the synthetic Ni sample retains its green color. The paper of Dumas et al. (2015b), based on the superior visibility of Ni in EXAFS spectroscopy with respect to Mg, aimed to first understand the genesis of Ni-rich talc from nucleation to crystal growth. All of the characterization methods showed a progressive structuration of talc with synthesis duration in a local order (FTIR, EXAFS) or in an extended (crystalline) order (XRD). The talc growth unit is constituted by 2−3 Ni-octahedra distanced from each other by 3.07 Å and 3−4 Si-

tetrahedra distributed on the top and bottom of the octahedral "sheet" and distanced from Ni by 3.29 Å. This "nano-talc" entity is the result of the talc precipitation. With the synthesis duration, these talc units get interlocked through the octahedral sheet. Simultaneously, the tetrahedral sheets grow, and Si−O−Si chains are progressively formed. At 300 °C in classic batch reactor or above the supercritical conditions, the synthesis time only influences the particle size at the local order. The mixing of starting material and its impact on the cationic distribution reveal that independently of the proto-talc preparation, a random distribution between octahedral cations is obtained at 300 °C. Contrary to previous literature (Decarreau et al., 1989), no cluster formation was evidenced at low temperatures.

Accessing a wide range of colors is possible just by the set of substitutions (Figure 15). Visual aspect can also be modified. For instance, synthetic Co-talcs (Figure 16) not only present the pearled and shiny aspect of natural talcs, but they form films that keep these visual properties after pressing (Figure 17). But, the most interesting is that this game of substitutions leads to products that may have some new physical characteristics such as low-temperature permanent magnetism for samples with Ni.

Remarkably, nano-divided mineral products can also be inserted in the surface to endow the particles with electrical conduction (Bonino et al., 2012) or magnetic properties. For example, synthetic talc particles bearing nano-magnetites on their borders have been obtained by a one-pot process (Dumas et al., 2011b). They display valuable magnetism at room temperature (Figure 18).

Dispersion in polymer matrix

In principle, the adsorption of various molecules, atoms and mineral phases can be envisaged in order to confer new chemical and physical properties to synthetic talcs. For instance, colored and/or fluorescent organic molecules have been successfully adsorbed on synthetic talc particles (Aymonier et al., 2017a, b). Of course, the amount of adsorbed species is much larger on synthetic talcs than on natural talcs, because of increased specific surface and extended borders where SiOH and MgOH groups favor hydrogen bonds and electrostatic interactions. Synthetic talcs thus present original physical behaviors and functionalities, which are highly sought after by manufacturers to develop new composite materials. Polymers are materials in which these nanoparticles are of particular interest. Indeed, introducing a small and well dispersed mineral filler allows the mechanical strength and/or other physical and chemical parameters of polymers to be improved. Many studies done with talcs and natural clays have first shown the interest of using these micronic mineral fillers. Recently a large number of polymer stability studies have been carried out using synthetic talcs fillers, and they have shown the superiority of these submicrometric particles.

To the best of our knowledge, no Ni-rich talc particles have been introduced in polymers. However, the following example suggests the possibility to do so. Using synthetic talc or Fe_3O_4-synthetic talc as filler in the synthesis of polyurethane by physical mixture, Dias et al. (2015, 2016) and Dos Santos et al. (2015) obtained nanocomposites in which the mineral filler was well dispersed into the polyurethane matrix even at high filler content of 10 wt.%. These composite materials showed superior crystallization temperature and thermal stability. Synthetic talc gel (Dias et al., 2018) and nano-Fe_3O_4-synthetic talc gel (Dos Santos et al., 2018) was also incorporated into a waterborne polyurethane (WPU) matrix, which is much more environmentally friendly than its solvent-based analogue. For example, in the case of nano-Fe_3O_4-synthetic talc gel, the obtained composite displayed a typical ferromagnetic behavior

below Curie temperature (about 120 K), a superparamagnetic behavior above this temperature and superior mechanical properties compared to solvent-based nanocomposites. Synthetic talcs manufactured in nano-gel form are particularly interesting because their interaction with water favors the dispersion of the fillers within the WPU matrix.

The high surface area of synthetic talc plays a significant role in the increase of crystallinity and thermal properties of the nanocomposites, provided that the nano-fillers are well dispersed/or exfoliated into the various polymer matrices. This is generally the case (Yousfi et al., 2013, 2014, 2015). But, the dispersion of nanometric charges is often difficult to measure without using expensive investigations techniques (SEM, TEM, AFM, …). Magnesium synthetic talc are white, just like the polymer matrices, and the submicrometer size makes the particles very difficult to observe by optical methods. A simple way is to replace Mg with Ni or with another divalent element, to access colored powder or gel(Prado et al., 2015).

Figure 19a shows a sample of polyurethane loaded with 10% Ni talc. The homogeneous green color suggests that the nano-charges are well dispersed. On the other hand, for the same concentration, in Figure 19b, a segregation of the nano-charges has taken place during the preparation of the polyurethane film, and the coloration is irregular. For low nano-charge concentrations, it can be observed with the naked eye that the dispersions of nano-charges are good in the matrix (Figure 19c).

Mineral synthesis: a link for understanding the Ni- and Co-rich lateritic environments

The interest of incorporating Ni, Co, or other divalent elements into talc is therefore obvious. However, the processes during crystal growth in synthesis are similar to natural processes. In natural environment, the Ni-rich mineral phases constituting the so-called garnierite Ni-ores are

dominated in most New Caledonia occurrences by talc-like minerals, also called kerolite or pimelite depending on the relative concentration of Mg and Ni. The Ni–Mg kerolite solid solution varies between the two end-members, e.g. Mg-rich kerolite to Ni-rich pimelite (Cathelineau et al., 2015, 2016, 2017; Myagkiy et al., 2017; Quesnel et al., 2017). Kerolite has a structure close to that of talc, with an interlayer distance of ~9.5Å, but it is characterized by an excess of Mg in the octahedral site and a relative deficit of Si in the tetrahedral site (Brindley et al., 1979). The H_2O content is also higher than in talc and an ideal chemical formula is : $(Ni,Mg)_{3+x}(Si_{4-y})O_{10}(OH)_2 \cdot nH_2O$, where x = 2y and n ~ 1.

The solid solution between the Ni and Mg end-members was complete without any gap, corresponding to a Ni–Mg substitution in the octahedral sheet. Raman spectra in the OH stretching vibration region have been recorded on representative samples from Ni-ores in New-Caledonia, covering the whole range of Ni–Mg substitution. This study shows a continuous and significant evolution from the Mg to the Ni end-member and reveals that four possible arrangements of Ni and Mg in the octahedral sheet are encountered, these arrangements being dependent on the Ni–Mg substitution rate. For synthetic talcs, the formula is identical but without the water molecules, the solid solutions are also complete and continuous (Martin et al. 1992, 1996, 1997; Martin, 1994; Petit et al., 2004a, b; Dumas, 2013c; Dumas et al., 2015b). The difference between talc and kerolites is very small, and the question is whether natural kerolites are more like synthetic talcs or synthetic proto-talcs. Substitutions, complete and continuous solid solutions between the Mg and Ni poles are arguments to say that the phenomena of the natural environment are similar to those of hydrothermal laboratory processes. . In both natural and synthetic cases, a random distribution was observed but no cluster distribution.

The similarities between the crystal growths in natural environment and in synthetic medium will prompt us to compare the three major phases, namely proto-talc, synthetic talc and natural

kerolites, in the course of further work. The results will be essential to clarify the synthesis processes during the transition to industrial production. Indeed, mineral fillers are enormously used because they allow the material qualities to be much improved, besides lowering the price of the material in which they are inserted. If the size of the conventional inorganic fillers is micronic or multi-micronic, the tests with nano-divided charges show an increase of certain properties if and only if these charges are uniformly distributed in the composite materials. The work on the new fillers can permit the production of the dozen patents filed by L'OREAL on these hydrophilic sub-micron charges that modify the rheology of certain preparations in comparison with those charged with hydrophobic natural minerals.

Acknowledgements:

The authors wish to acknowledge the financial support from IMERYS Company for the PhD. grants of Marie Claverie and Mathilde Poirier and CAPES (Brazil government) for PhD scholarship of Manoela Argenton Prado, and Guilherme Dias and CNPq for DT grant (number 303467/2015-0).

References:

Arseguel, D., Bonino, J.-P., Decarreau, A., Ferrage, E., Ferret, J., Grauby, O., Lebre, C., Martin, F., Petit, S. (2006) Method for preparing talcose compositions comprising synthetic mineral particles containing silicon, germanium and metal. Patents FR2903680, WO2008009799.

Aymonier, C., Erriguible, A., Marre, S., Serani, A., Cansell, F. (2007) Processes using supercritical fluids: a sustainable approach for the design of functional nanomaterials. International Journal of Chemical Reactor Engineering 5, A77.

Aymonier, C., Dumas, A., Le Roux, C., Martin, F., Micoud, P., Poirier M., Slostowski, C. (2014) Process for the continuous preparation of phyllomineral synthetic particles. Patents FR3019813, WO2015159006.

Aymonier, C., Fery-Forgues, S., Le Roux, C., Martin, F., Micoud, P., Poirier M. (2017a) Coloured organic/inorganic hybrid materials and method for preparing same. Patents FR3062074, WO2018138148.

Aymonier, C., Fery-Forgues, S., Le Roux, C., Martin, F., Micoud, P., Poirier M. (2017b) Photoluminescent hybrid organic/inorganic materials and method for preparing same. Patent FR3062073, WO2018138153.

Baba, A.A., Ibrahim, A.S., Bale, R.B., Adekola, F.A., Alabio, A.G.F. (2015) Purification of a Nigerian talc ore by acid leaching. Applied Clay Science 114, 476-483. DOI: 10.1016/j.clay.2015.06.031.

Bacchin, P., Bonino, J.P., Martin, F., Combacau, M., Barthes, P., Petit, S., Ferret, J. (2006) Surface pre-coating of talc particles by carboxyl methyl cellulose adsorption: Study of adsorption and consequences on surface properties and settling rate. Colloids and Surfaces A: Physicochemical and Engineering Aspects, 272, 211-219. DOI: 10.1016/j.colsurfa.2005.07.026.

Bonino, J. P., Bacchin, P., Martin, F., Barthes, P., Ferrage, E., Vautrin, W., Vaillant, S. (2002) Composite material consisting of a metal matrix and talc. Patent FR2848219, WO2004063428.

Borges, R., Dutra, L.M., Barison, A., Wypych, F. (2016) MAS NMR and EPR study of structural changes in talc and montmorillonite induced by grinding. Clay Minerals 51, 69-80. DOI: 10.1180/claymin.2016.051.1.06.

Brindley, G.W., Bish, D.L., Wan, H.M. (1979) Compositions, structures, and properties of nickel-containing minerals in the kerolite-pimelite series. American Mineralogist 64, 615-625.

Cansell, F., Aymonier, C. (2009) Design of functional nanostructured materials using supercritical fluids. Journal of Supercritical Fluids 47, 508-516. DOI: 10.1016/j.supflu.2008.10.002.

Castillo L.A., Barbosa, S.E., Maiza P., Capiati N.J. (2014) Integrated process for purification of low grade talc ores 32, 1-7. DOI: 10.1080/02726351.2012.755588.

Cathelineau, M., Caumon, M. C., Massei, F. Brie, D., Harlaux, M. (2015) Raman spectra of Ni-Mg kerolite: effect of Ni-Mg substitution on O-H stretching vibrations. Journal of Raman Spectroscopy 46, 10, 933-940. DOI: 10.1002/jrs.4746.

Cathelineau, M., Quesnel, B., Gautier, P., Boulvais, P., Couteau, C., Drouillet, M. (2016) Nickel dispersion and enrichment at the bottom of the regolith: formation of pimelite target-like ores in rock block joints (Koniambo Ni deposit, New Caledonia). Mineralium Deposita 51, 2, 271-282. DOI: 10.1007/s00126-015-0607-y.

Cathelineau, M., Myagkiy, A., Quesnel, B., Boiron, M.C., Gautier, P., Boulvais, P., Ulrich, M., Truche, L., Golfier, F., Drouillet, M. (2017). Multistage crack seal vein and hydrothermal Ni enrichment in serpentinized ultramafic rocks (Koniambo massif, New Caledonia). Mineralium Deposita 52, 7, 945-960. DOI: 10.1007/s00126-016-0695-3.

Cavajda, V., Uhlik, P., Derkowski, A., Caplovicova, M., Madejova, J., Mikula, M. Ifka, T. (2015) Influence of grinding and sonication on the crystal structure of talc. Clays and Clay Minerals 63, 4, 311-327. DOI: 10.1346/CCMN.2015.0630405.

Chabrol, K., Gressier, M., Pebere, N., Menu, M.J., Martin, F., Bonino, J.P., Marichal, C., Brendle, J. (2010) Functionalization of synthetic talc-like phyllosilicates by alkoxyorganosilane grafting. Journal of Materials Chemistry 20, 9695-9706. DOI: 10.1039/c0jm01276a.

Claverie, M., Dumas, A., Carême, C., Poirier, M., Le Roux, C., Micoud, P. Martin, F., Aymonier, C. (2018) Synthetic talc and talc-like structures: preparation, features and applications. Chemistry: A European Journal 24, 519-542. DOI: 10.1002/chem.201702763.

Corona, J.C., Jenkins, D.M., Dyar, M.D. (2015) The experimental incorporation of Fe into talc: a study using X‐ray diffraction, Fourier transform infrared spectroscopy, and Mössbauer spectroscopy. Contributions to Mineralogy and Petrology 170, 29. DOI: 10.1007/s00410-015-1180-1.

Decarreau, A., Mondesir, H., Besson, G. (1989) Synthesis and stability of Mg and Ni stevensite, kerolite and talcs between 80°C and 240°C. Comptes Rendus de l'Académie des Sciences, Série II 308, 301–306.

Dellisanti, F., Valdre, G., Mondonico, M. (2009) Changes of the main physical and technological properties of talc due to mechanical strain. Applied Clay Science 42, 398-404. DOI: 10.1016/j.clay.2008.04.002.

Dias, G., Prado, M.A., Carone, C., Ligabue, R., Dumas, A., Martin, F., Le Roux, C., Micoud, P., Einloft, S. (2015) Synthetic silico-metallic mineral particles (SSMMP) as nanofillers: comparing the effect of different hydrothermal treatments on the PU/SSMMP nanocomposites properties. Polymer Bulletin 72, 11, 2991-3006. DOI: 10.1007/s00289-015-1449-6.

Dias, G., Prado, M., Carone, C., Ligabue, R., Dumas, A., Le Roux, C., Micoud, P., Martin, F., Einloft, S. (2016) Comparing different synthetic talc as fillers for polyurethane nanocomposites. Macromolecular Symposia 367, 136-142. DOI: 10.1002/masy.201500141.

Dias, G., Prado, M., Le Roux, C., Poirier, M., Micoud, P., Ligabue, R., Martin, F., Einloft, S. (2018) Analyzing the influence of different synthetic talcs in waterborne polyurethane

nanocomposites obtainment. Journal of Applied Polymer Science 135, 14, 46107. DOI: 10.1002/app.46107.

Dietemann, M. (2012) Etude de la précipitation du silicate de magnésium amorphe assistée par ultrasons: synthèse, caractérisation et modélisation. PhD thesis, University of Toulouse - INP, France.

Dietemann, M., Baillon, F., Espitalier, F., Calvet, R., Accart, P., Del Confetto, S., Greenhill-Hooper, M. (2013) Evaluation of the physico-chemical properties of an amorphous magnesium silicate synthesized by an ultrasound-assisted precipitation. Chemical Engineering Journal 215-216, 658-670. DOI: 10.1016/j.cej.2012.11.079.

Dos Santos, L.M., Ligabue, R., Dumas, A., Le Roux, C., Micoud, P., Meunier, J.F., Martin, F., Einloft, S. (2015) New magnetic nanocomposites: Polyurethane / Fe_3O_4-synthetic talc. European Polymer Journal 69, 38-49. DOI: 10.1016/j.eurpolymj.2015.05.026.

Dos Santos, L.M., Ligabue, R., Dumas, A., Le Roux, C., Micoud, P., Meunier, J.F., Martin, F., Corvo, M., Almeida, P., Einloft, S. (2018) Waterborne polyurethane/Fe_3O_4-synthetic talc composites: synthesis, characterization, and magnetic properties. Polymer Bulletin 75, 1915-1930. DOI 10.1007/s00289-017-2133-9.

Dublet, G., Juillot, F., Brest, J., Noël, V, Fritsch, E., Proux, O., Olivi, L., Ploquin, F., Morin, G. (2017) Vertical changes of the Co and Mn speciation along a lateritic regolith developed on peridotites (New Caledonia). Geochimica and Cosmochimica Acta 217, 1-15. DOI: 10.1016/j.gca.2017.07.010.

Dumas, A., Le Roux, C., Martin, F., Micoud, P. (2011a) Process for preparing a composition comprising synthetic mineral particles and composition. Patents FR2977580, WO2013004979.

Dumas, A., Gardes, E., Le Roux, C., Martin, F., Micoud, P. (2011b) Process for preparing a magnetic talcous composition and magnetic talcous composition. Patents FR2984872, WO2013093376.

Dumas, A., Martin, F. Ferrage, E., Micoud, P., Le Roux, C., Petit, S. (2013a) Synthetic talc advances: coming closer to nature, added value and industrial requirements. Applied Clay Science 85, 8–18. DOI: 10.1016/j.clay.2013.09.006.

Dumas, A., Martin, F., Le Roux, C., Micoud, P., Petit, S., Ferrage, E., Brendle, J., Grauby, O., Greenhill-Hooper, M. (2013b) Phyllosilicates synthesis: a way of accessing edges contributions in NMR and FTIR spectroscopies. Example of synthetic talc. Physics and Chemistry of Minerals 40, 361–373. DOI: 10.1007/s00269-013-0577-5.

Dumas, A. (2013c) Elaboration de nouveaux procédés de synthèse et caractérisation de talcs sub-microniques : de la recherche fondamentale vers des applications industrielles. PhD Thesis, University of Toulouse III - Paul Sabatier, France.

Dumas, A., Martin, F., Ngo Ke, T., Nguyen Van, H., Nguyen Viet, D., Nguyen Tat, V., Kieu Quy, N., Micoud, P., de Parseval, P. (2015a) The crystal-chemistry of Vietnamese talcs from the Thanh Son district (Phu Tho province, Vietnam). Clay Minerals 50, 607-617. DOI: 10.1180/claymin.2015.050.5.05.

Dumas, A., Mizrahi, M., Martin, F., Requejo F.G. (2015b) Local and extended-order evolution of synthetic talc during hydrothermal synthesis: extended X‑ray absorption fine structure, X‑ray diffraction, and Fourier transform infrared spectroscopy studies. Crystal Growth and Design 15, 5451−5463. DOI: 10.1021/acs.cgd.5b01076.

Dumas, A., Claverie, M., Slostowski, C., Aubert, G., Careme, C., Le Roux, C., Micoud, P., Martin, F., Aymonier, C. (2016) Fast-geomimicking using chemistry in supercritical water. Angewandte Chemie International Edition 55, 9868-9871, DOI: 10.1002/anie.201604096.

Godet, L. (2001) Broyage fin du talc par jets d'air opposés. PhD thesis, University of Lorraine - INPL, France.

Kloprogge, J.T., Komarneni, S., Amonette, J.E. (1999) Synthesis of smectite clay minerals: a critical review. Clays and Clay Minerals 47, 529–554. DOI: 10.1346/CCMN.1999.0470501.

Kojima, Y., Usuki, A., Kawasumi, M., Okada, A., Fukushima, Y., Kurauchi, T., Kamigaito, O. (1993a) Mechanical properties of Nylon-6 clay hybrid. Journal of Materials Research 8, 1185–1189. DOI: 10.1557/JMR.1993.1185.

Kojima, Y., Usuki, A., Kawasumi, M., Okada, A., Kurauchi, T., Kamigaito, O. (1993b) Sorption of water in Nylon-6 clay hybrid. Journal of Applied Polymer Science 49, 1259–1264. DOI: 10.1002/app.1993.070490715.

Lèbre, C. (2007) Elaboration et caractérisation de talcs synthétiques pour l'amélioration des propriétés physiques des matériaux composites industriels. PhD thesis, University of Toulouse III - Paul Sabatier, France.

Le Roux, C., Martin, F., Micoud, P., Dumas, A. (2010) Method for preparing a composition including synthetic inorganic particles. Patents FR2969594, WO2012085239.

Liao, J., Senna, M. (1992) Thermal behavior of mechanically amorphized talc. Thermochimica Acta 197, 295-306.

Martin, F., Petit, S., Grauby, O., Noack, Y., Hazemann J.L., Decarreau, A. (1992) Experimental study of Si-Ge tetrahedral solid solution in Ni-Co-Mg talcs. Thin Solid Films 222, 189-195.

Martin, F. (1994) Etude cristallographique et cristallochimique de l'incorporation du Germanium et du Gallium dans les phyllosilicates : approche par synthèse minérale. PhD thesis, University of Aix-Marseille, France.

Martin, F., Ildefonse, P., Hazemann, J.L., Petit, S., Grauby, O., Decarreau, A. (1996) Random distribution of Ge and Si in synthetic talc: an EXAFS and FTIR study. European Journal of Mineralogy 8, 289-299.

Martin, F., Ferret, J., Lèbre, C., Petit, S., Grauby, O., Bonino, J.P., Arseguel, D., Decarreau, A., Ferrage, E. (2006) Method for preparing a synthetic talc composition from a kerolite composition. Patents FR2903682, WO2008009801.

Misch, D., Pluch, H., Mali, H., Ebner, F., Hui, H. (2018) Genesis of giant Early Proterozoic magnesite and related talc deposits in the Mafeng area, Liaoning Province, NE China. Journal of Asian Earth Sciences 160, 1-12. DOI: 10.1016/j.jseaes.2018.04.005.

Myagkiy, A., Truche, L., Cathelineau, M., Golfier, F. (2017) Revealing the conditions of Ni mineralization in the laterite profiles of New Caledonia: insights from reactive geochemical transport modelling. Chemical Geology 466, 274-284. DOI: 10.1016/j.chemgeo.2017.06.018.

Petit, S., Robert, J.L., Decarreau, A., Besson, G., Grauby, O., Martin, F. (1995) Contribution of spectroscopic methods to 2:1 clay characterization. Bulletin des Centres de Recherches Exploration-Production Elf-Aquitaine, 19, 1, 119-148.

Petit, S., Decarreau, A., Martin, F., Buchet, R. (2004a) Refined relationship between the position of the fundamental OH stretching and the first overtones for clays. Physics and Chemistry of Minerals 31, 585-592. DOI 10.1007/s00269-004-0423-x.

Petit, S., Martin, F., Wiewiora, A., de Parseval, P., Decarreau, A. (2004b) Crystal-chemistry of talc: a near infrared (NIR) spectroscopy study. American Mineralogist 89, 319-326. DOI: 10.2138/am-2004-2-310.

Prado, M.A., Dias, G., Carone, C., Ligabue, R., Dumas, A., Le Roux, C., Micoud, P., Martin, F., Einloft, S. (2015) Synthetic Ni-talc as filler for producing polyurethane nanocomposites. Journal of Applied Polymer Science 132, 16, 41854. DOI: 10.1002/app.41854.

Quesnel, B., Le Carlier de Veslud, C., Boulvais, P., Gautier, P., Cathelineau, M., Drouillet, M. (2017) 3D modeling of the laterites on top of the Koniambo Massif, New Caledonia: refinement of the per descensum lateritic model for nickel mineralization. Mineralium Deposita 52, 7, 961-978. DOI: 10.1007/s00126-017-0712-1.

Reveron, H., Elissalde, C., Aymonier, C., Bousquet, C., Maglione, M., Cansell, F. (2006) Continuous supercritical synthesis and dielectric behaviour of the whole BST solid solution. Nanotechnology 17, 3527–3532. DOI: 10.1088/0957-4484/17/14/028.

Robert, J.F., Fragnier, P. (1996) Talc production: an overview. Macromolecular Symposia 108, 13–18. DOI: 10.1002/masy.19961080104.

Sanchez-Soto, P.J., Wiewiora, A., Aviles, M.A., Justo, A., Perez-Maqueda, L.A., Perez-Rodriguez, J.L., Bylina, P. (1997) Talc from Puebla de Lillo, Spain. II. Effect of dry grinding on particle size and shape. Applied Clay Science 12 (4), 297-312. DOI: 10.1016/S0169-1317(97)00013-6.

Soriano., M., Melgosa, M., Sanchez-Maranon, M., Delgado, G., Gamiz, E., Delgado, R. (1998) Whiteness of talcum powders as a quality index for pharmaceutical uses. Color Research and Application 23, 3, 178–185.

Soriano., M., Sanchez-Maranon, M., Melgosa, M., Gamiz, E., Delgado, R. (2002) Influence of chemical and mineralogical composition on color for commercial talcs. Color Research and Application 27, 6, 430–440. DOI: 10.1002/col.10096.

Usuki, A., Kawasumi, M., Kojima, Y., Okada, A., Kurauchi, T., Kamigaito, O. (1993a) Swelling behavior of montmorillonite cation exchanged for omega-amino acids by epsilon-caprolactam. Journal of Materials Research 8, 5, 1174–1178. DOI: 10.1557/JMR.1993.1174.

Usuki, A., Kojima, Y., Kawasumi, M., Okada, A., Fukushima, Y., Kurauchi, T., Kamigaito, O., (1993b) Synthesis of nylon-6 clay hybrid. Journal of Materials Research 8, 5, 1179–1184. DOI: 10.1557/JMR.1993.1179.

Yousfi, M., Livi, S., Dumas, A., Le Roux, C., Crépin-Leblond, J., Greenhill-Hooper, M., Duchet-Rumeau, J. (2013) Use of new synthetic talc as reinforcing nanofillers for polypropylene and polyamide 6 systems: thermal and mechanical properties. Journal of Colloid and Interface Science 403, 29-42. DOI: 10.1016/j.jcis.2013.04.019.

Yousfi, M., Livi, S., Dumas, A., Crépin-Leblond, J., Greenhill-Hooper, M., Duchet-Rumeau, J. (2014) Compatibilization of polypropylene/polyamide 6 blends using new synthetic nanosized talc fillers: morphology, thermal, and mechanical properties. Journal of Applied Polymer Science 131, 13, 40453. DOI: 10.1002/app.40453.

Yousfi, M., Livi, S., Dumas, A., Crépin-Leblond, J., Greenhill-Hooper, M., Duchet-Rumeau, J. (2015) Ionic compatibilization of polypropylene/polyamide 6 blends using an ionic liquids/nanotalc filler combination: morphology, thermal and mechanical properties. RSC Advances 5, 57, 46197–46205. DOI: 10.1039/c5ra00816f.

Zazenski, R., Ashton, W.H., Briggs, D., Chudkowski, M., Kelse, J.W., MacEachern, L., McCarthy, E.F., Nordhauser, M.A., Roddy, M.T., Teetsel, N.M., Wells, A.B., Gettings, S.D.

(1995) Talc – occurrence, characterization, and consumer applications. Regulatory Toxicology and Pharmacology 21, 2, 218–229. DOI: 10.1006/rtph.1995.1032.

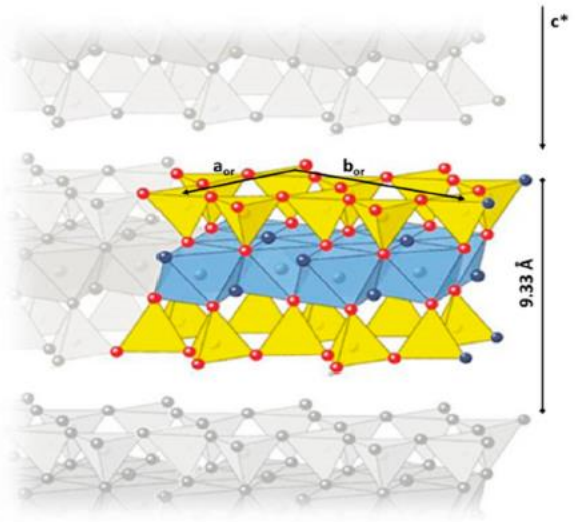

Fig. 1. Structure of talc (2:1 phyllosilicate); yellow ball: silicon; light blue ball: magnesium; dark blue ball: hydroxide; red ball: oxygen. (For interpretation of the references to color in this figure legend, the reader is referred to the web version of this article.)

Fig. 2. Different batch type reactors from 350 to 2000 cc for temperatures ranging from 0 to 500 °C and maximum pressures of 300 bar.

Fig. 3. 18 L batch reactor implanted at GET and owned by IMERYS.

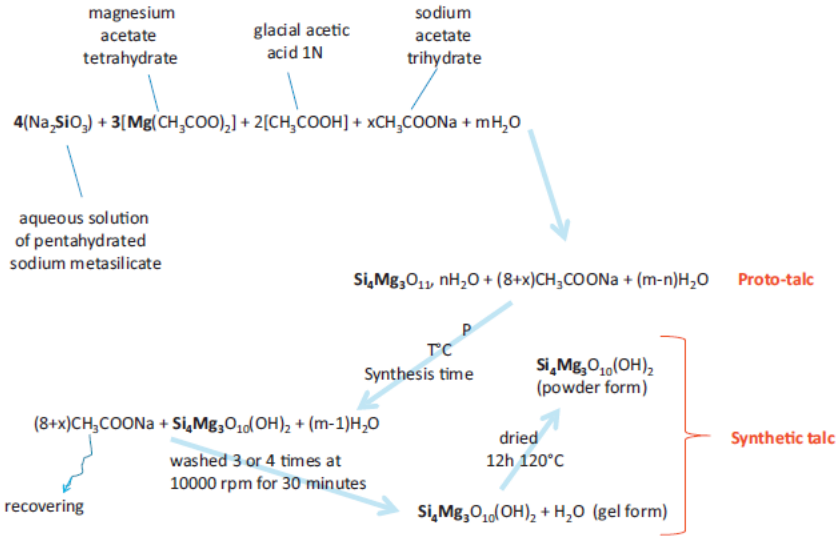

Fig. 4. Reaction of precipitation leading to the formation of proto-talc and then to the synthesis of talc.

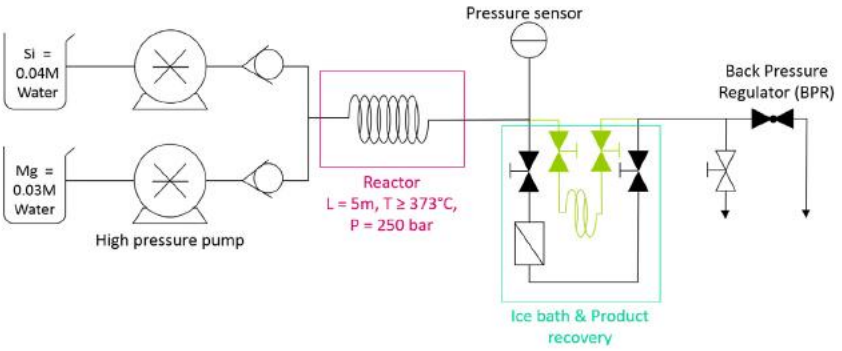

Fig. 5. Conceptual diagram of the phyllosilicate synthesis in continuous mode under supercritical conditions.

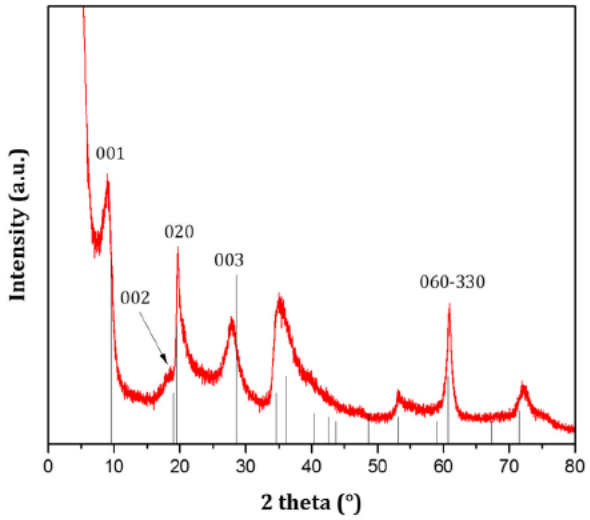

Fig. 6. X-ray diffractogram of a talc synthesized in supercritical water for a time of 20 s. Red: synthetic talc. Black: X-ray lines of natural talc. (For interpretation of the references to color in this figure legend, the reader is referred to the web version of this article.)

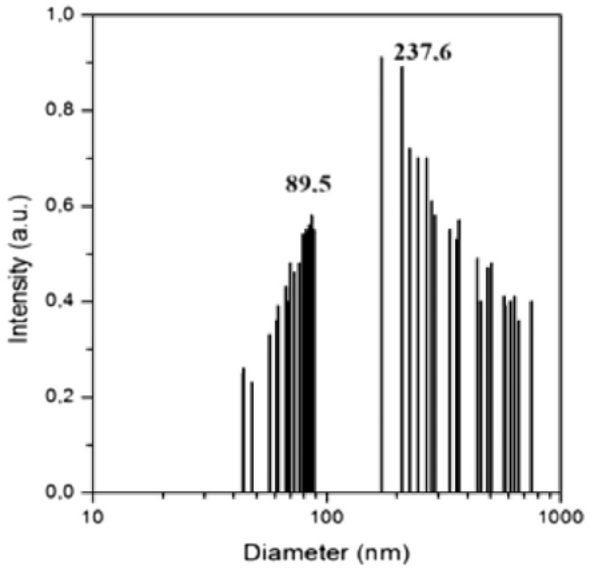

Fig. 7. Particle size distribution of a talc synthesized in supercritical water for a time of 20 s.

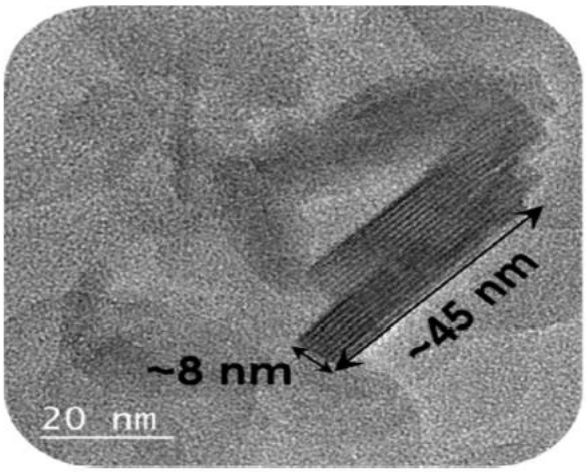

Fig. 8. Transmission electron microscopy image of a talc synthesized in supercritical water for a time of 20 s.

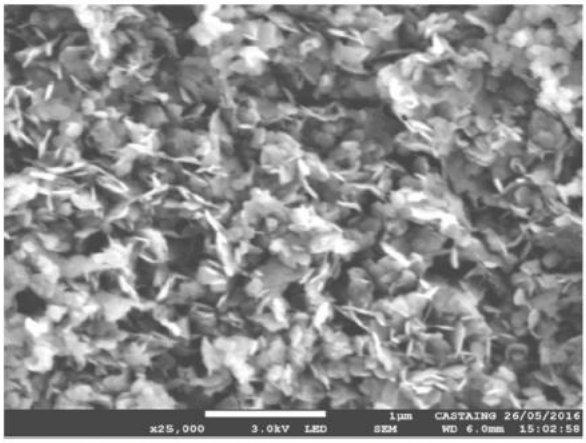

Fig. 9. Scanning electron microscope image of a talc synthesized in supercritical water for a time of 20 s.

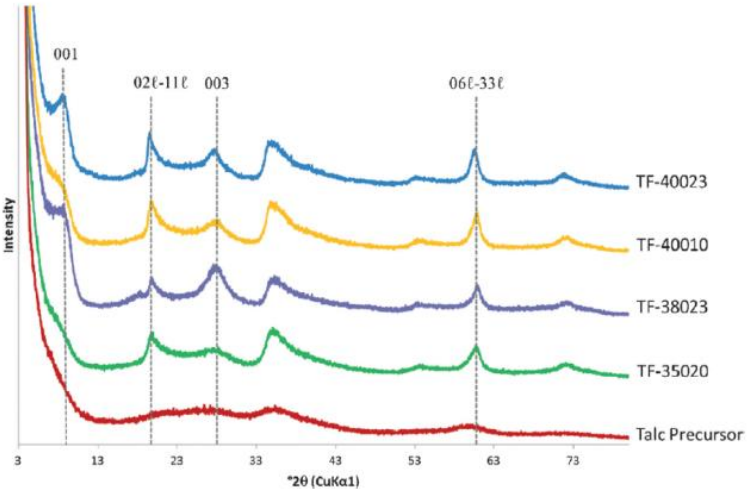

Fig. 10. XRD patterns of synthetic talc samples obtained using the supercritical hydrothermal flow synthesis process. XRD patterns of samples obtained by varying temperature (350 °C (green), 380 °C (purple), 400 °C (yellow and blue)), or synthesis time (10 s (yellow) and 20 or 23 s (green, purple, and blue)). The XRD of proto-talc (red) is named as talc precursor. From Dumas et al. (2016). (For interpretation of the references to color in this figure legend, the reader is referred to the web version of this article.)

Fig. 11. Synthetic talc powder (left) and aqueous gel of synthetic talc (right).

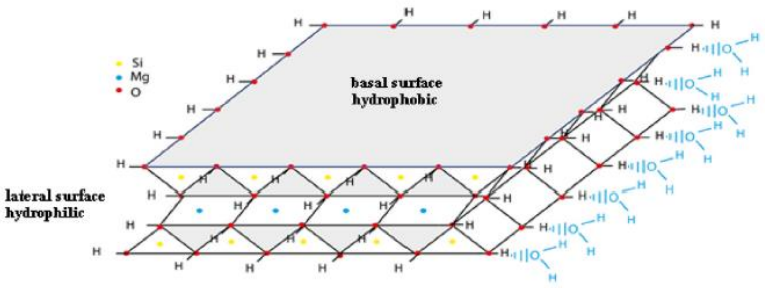

Fig. 12. Diagram of hydrophilic borders and hydrophobic surfaces of synthetic talc. The scheme has sizes of 4 nm^2 of area over 1 nm thick and is not the representation of a synthesized particle (size at least 10 times larger in the (ab) plane).

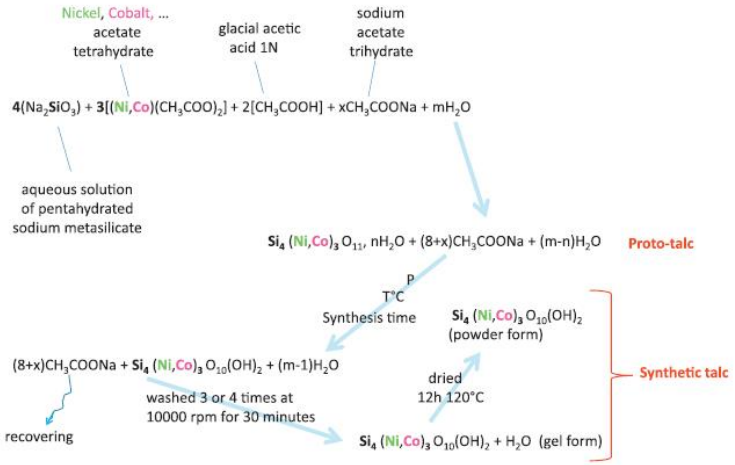

Fig. 13. Reaction precipitation leading to the formation of (Ni, Co, ...)-bearing proto-talc and then to the synthesis of (Ni, Co, ...)-bearing talc.

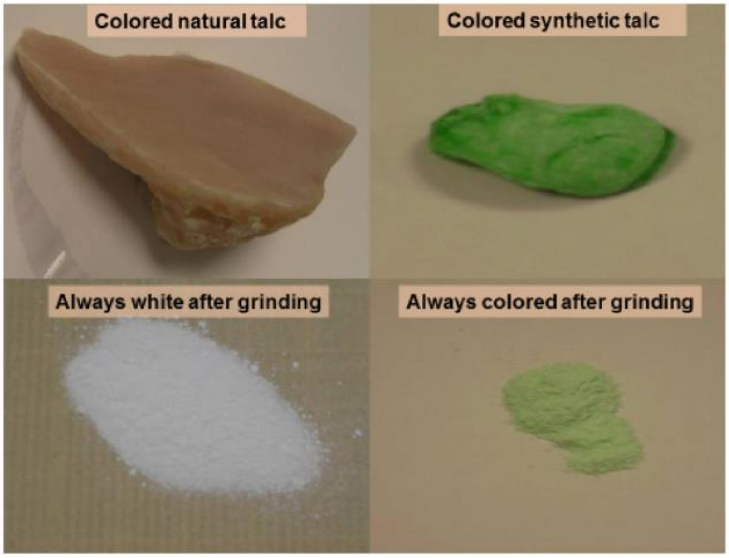

Fig. 14. Pink natural talc (left) and green synthetic talc (right) and their respective powder after grinding. (For interpretation of the references to color in this figure legend, the reader is referred to the web version of this article.)

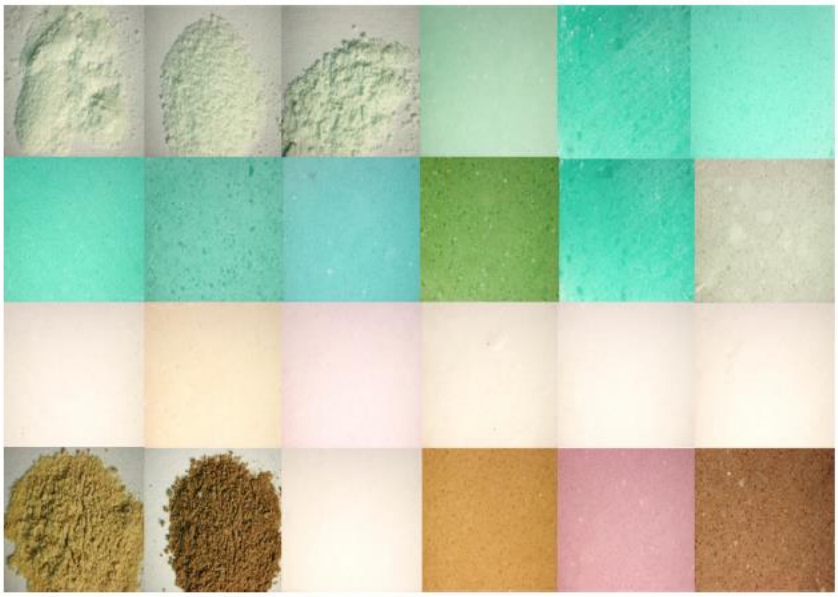

Fig. 15. Examples of synthetic talc colors by partial or complete substitution of magnesium by others divalent cations.

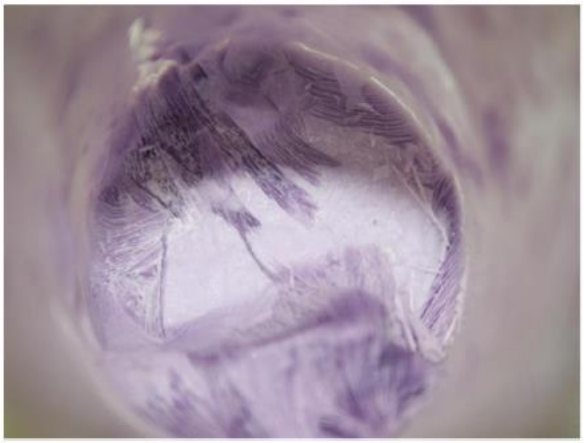

Fig. 16. Co-bearing talc with shiny appearance.

Fig. 17. Pearl film of Ni-Mg-bearing talc.

Fig. 18. Magnetic synthetic talc attracted by the magnet. Note that all the powder is attracted to the magnet.

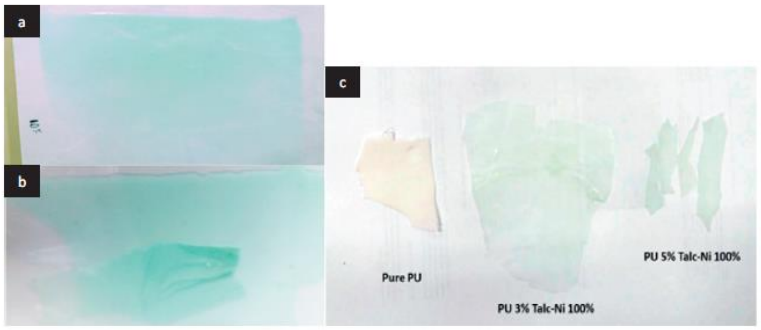

Fig. 19. Polyurethane films with various Ni-bearing talc contents: a) homogeneous distribution of nano-charges; b) heterogeneous distribution of nano-charges; c) films containing low talc charge.